Interactions of -Tocopherol in F127/lignin microemulsions: A DFT and semi-empirical study

(Article begins on next page)

18 May 2024

Interactions of α-Tocopherol in F127/lignin microemulsions: A DFT and semi-empirical study

Pouya Karimi [a],[**], Abbas Rahdar [b], Francesco Baino [c],[*]

[a] *Department of Chemistry, Faculty of Sciences, University of Zabol, Zabol, Iran*
[b] *Department of Physics, School of Basic Sciences, University of Zabol, Zabol, Iran*
[c] *Institute of Materials Physics and Engineering, Department of Applied Science and Technology, Politecnico di Torino, Torino, Italy*

ARTICLE INFO

ABSTRACT

Tocopherols are fat soluble substances with antioxidant properties. The α-Tocopherol (T) is the major form of Tocopherols and can decrease the risk of cancer. F127-based and Lignin-based oil-in-water microemulsions seem to increase the bioavailability of T and cause better release of this therapeutic agent. Thus, T-loaded micro-emulsions were designed by means of density functional theory (DFT) and semi-empirical methods. Atoms in molecules (AIM), natural bond orbital (NBO) analyses, localized molecular orbital energy decomposition analysis (LMO-EDA), and density of states plots were employed to explore the effective factors on the strength of the interactions between surfactants and T. Results indicate that F127-T complexes are more stable than Lignin-T ones. Furthermore, the stable release of T in microemulsions is due to the electrostatic interactions between surfactants and T. Formation of hydrogen bond (HB) interactions between surfactants and T stabilizes the microemulsion system. These interplays are suggested to take part in the better function of T in microemulsions compared to free T. The semi-empirical study reveals that the heats of formation (ΔH_f values) of the F127-T complexes are less negative than those for the Lignin-T ones.

1. Introduction

Tocopherols, commonly known as belonging to the vitamin E group, are hydrophobic drugs with wide pharmaceutical applications [1–3]. The main sources of Tocopherols are vegetable oils [4]. These drugs are proposed to diminish the risk of cancer due to their antioxidant features [5]. The α-Tocopherol (T) is the most important form of these drugs and is considered as the classic vitamin E [6]. Therefore, design of safe T-drug delivery systems is appealing for therapeutic purposes.

Some authors focused on α-Tocopherol-loaded polymeric nano-particles and showed that these systems have lower toxicity and higher anti-oxidative protection against H_2O_2 [7]. Also, the targeted delivery of surface-modified α-Tocopherol from 5-flurouracil-loaded poly(D,L-lac-tic-*co*-glycolic acid) (PLGA) nanoparticles has been studied [8]. More-over, antioxidant activity and efficacy of Tocopherol-loaded transfersomes have been previously studied and results revealed good potential of these topical delivery system [9]. Encapsulation efficiencies of α-Tocopherol-loaded poly(ε-caprolactone) (PCL) nanoparticles have been tested by changing solvent, concentration, and ultrasonication

time [10]. Some scientists also reported that α-Tocopherol-loaded chitosan-based copolymers have good potential as wound dressing ma-terials and stimulate the healing process [11]. It was shown that the bioavailability of α-Tocopherol can be improved when it is delivered from pure PLGA and chitosan-coated PLGA nanoparticles [12]. Also, α-Tocopherol loaded in liposomes can help to increase solubility of vitamin E and to protect spermatozoa during cryopreservation [13]. Magnetic nanoparticles have also been used for the co-delivery of doxorubicin and D-α-Tocopherol polyethylene glycol 1000 succinate (vitamin E TPGS) [14].

Alternatively, vitamin E can be incorporated in microemulsions. For example, a water-in-oil microemulsion containing vitamin A and α-tocopherol has been recently developed that has additive effect against acute skin inflammation [15]. In general, surfactant-stabilized oil-in-water microemulsions are known as good nano-carrier systems for the delivery of hydrophobic drugs with higher bioavailability, lower toxicity, and lower side effects [16–21]. In this regard, Pluronics (non-ionic surfactants) are better in nano-colloidal systems of oil-in-water microemulsion as a result of higher stability and less

---

toxicity in comparison to ionic surfactants [22,23]. Results of previous studies revealed that the solubility, stability, bioavailability, and effective release of T are improved by the inclusion of drug into oil-in-water microemulsion [24,25].

Copolymers such as PEO−PPO−PEO (poly(ethylene oxide)−poly (propylene oxide)− poly(ethylene oxide) have low toxicity [26]. Thus, these Pluronic-type stabilizing agents can be applied for the encapsulation of hydrophobic drugs within oil-in-water microemulsions. Pluronic F127 is a useful copolymer that may act as an encapsulation material [27]. Previously, application of F127 in drug delivery strategies have been reported [28–34].

Another attractive encapsulating substance is lignin, which is a renewable bioresource for manufacturing various materials such as detergents and dispersants [35]. This green surfactant has biomedical applications [36,37] and can improve the release rate of various drugs [38,39]. Lignin-based hollow nanoparticles have also been used for the drug delivery [40,41]. Lignin-drug microemulsions have been formerly applied as good drug carriers with high encapsulation efficiency [42–44].

Experimental analyses of the drug delivery systems give helpful outcomes. However, investigation of intra- and intermolecular interactions at the molecular level is very complicated or even impossible by experimental examinations. On the other hand, computational quantum chemistry methods provide informative results about atomic/molecular interactions in these systems [32,34,and 45]]. Thus, computational investigations can complement experimental efforts. In this study, interactions of T with F127 and lignin are considered to get better insight about the nature of interactions of this drug with the mentioned surfactants. Geometries, energy data, strength of interactions, charge transfer (CT), properties of electron charge densities, donor-acceptor stabilizing energies, density of states (DOS) plots, and localized molecular orbital energy decomposition analysis (LMO-EDA) were assessed to explore the effective factors that contribute in stabilizing the complexes of T with F127 and lignin.

2. Computational methods

Geometries of the T, F127, lignin, and binary complexes were optimized at the B3LYP/6-31G(d,p) level of theory via Gaussian09 program package [46]. The B3LYP method has good performance in calculating the relative HB energies and describing HB interactions [47,48]. Also, calculations were performed with PBEKCIS method at the 6–311++G(d, p) basis set.

Interaction energy of each binary complex that includes drug and surfactant is estimated as follows:

$$\Delta E = E_{complex} - (E_{drug} + E_{surfactant}) \qquad (1)$$

The electron charge densities and related properties were studied by atoms in molecules (AIM) method using AIM2000 program [49]. Population analyses were executed by natural bond orbital (NBO) method [50] using NBO program [51] that was implemented in Gaussian09 at the same level of theory. The NBO method considers charge transfers between filled donor molecular orbitals and empty acceptor ones. Energetic weights of the mentioned orbitals were evaluated by second-order perturbation theory. Stabilization energy ($E^{(2)}$) is calculated using Fock operator for donor orbital φi and acceptor orbital φj in each donor–acceptor interplay as:

$$E^{(2)} = \frac{|<\varphi_i|\hat{F}|\varphi_j>|^2}{\varepsilon_i - \varepsilon_j} \qquad (2)$$

Eigenvalues of the donor orbital and acceptor orbital were εi and εj, respectively.

Aromaticity of the six-member ring of T was evaluated by means of Para-delocalization index (PDI) scale [52]. The PDI is the mean value of para-delocalization in six-member rings and quantifies the local

aromaticity related to three para-positions explicitly, i.e. (1,4), (2,5), and (3,6), as follows:

$$PDI = \frac{\delta(1,4) + \delta(2,5) + \delta(3,6)}{3} \qquad (3)$$

The δ(A,B) is achieved from the double integration of the exchange-correlation density over the atomic basins in the AIM theory.

Semi-empirical methods have been parameterized to include all thermochemical corrections to obtain heat of formations. Thus, semi-empirical calculations were carried out using AM1 method [53] to better consider HB interactions.

3. Results and discussion

3.1. Geometries and energy data

The α-Tocopherol encompasses a methylated phenol ring [54], and the O–H bond in the mentioned ring is weaker compared to most other phenols. This weak bond allows donating a hydrogen atom to free radicals or contributes in forming hydrogen bond (HB) interactions with other species. The molecular structure of this drug is shown in Fig. 1.

Thus, it seems that formation of HB interactions between nanocarrier systems and T plays an important role on the efficiency of drug delivery process. Structures of the F127-drug and lignin-drug complexes were designed using GaussView 5.1 and optimized with Gaussian09. Results indicate that six stable hydrogen-bonded complexes are formed between surfactants and T. As shown in Fig. 2, these complexes are formed via intermolecular HB interactions between O–H group at phenol ring of drug (as hydrogen bond donor) and oxygen atoms of F127 or lignin (as hydrogen bond acceptor). Atoms that contribute in these interplays are O_1, H_2, and O_3. Binding energy (BE) values of the complexes are gathered in Table 1. BE is measured as –ΔE. Usually, BE is representative of the strength of the intermolecular interactions [55–58].

As shown in Table 1, BE values of the F127-T complexes are larger than those for the Lignin-T ones. Thus, HB interactions of F127 with T are stronger than those with lignin. Furthermore, hydrogen bond length (d_{HB}) values in the F127-T complexes are shorter than those in the Lignin-T ones. Energies related to highest occupied molecular orbital (HOMO) and lowest unoccupied molecular orbital (LUMO), as well as energy gap (EG) values of the complexes are also presented in Table 1. The EG value for the F127 and lignin is 8.629 and 5.758 eV, respectively. Results reveal that EG values of the complexes are smaller than those for the F127 and lignin. In fact, complex formation leads to decrease of EG values. The six member-ring of T is denoted with A. This phenol ring is considered as the center of reactions due to its capability in hydrogen donation to F127 and lignin. Changes of atomic charges, properties of electron charge densities, and aromaticity at this ring seem to be caused by intermolecular HB interactions influence on the stability of the F127-T and Lignin-T complexes. Thus, analyses of atomic charges and other molecular descriptors are presented in the next sections to find a relationship between BE values of the complexes and these descriptors.
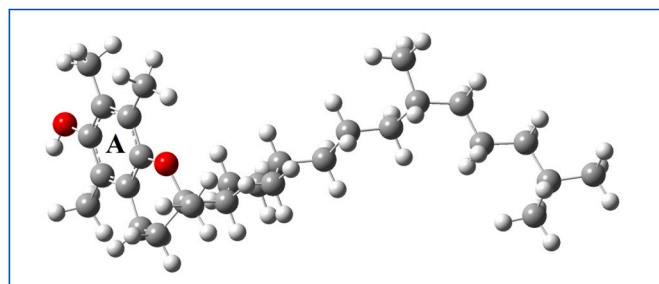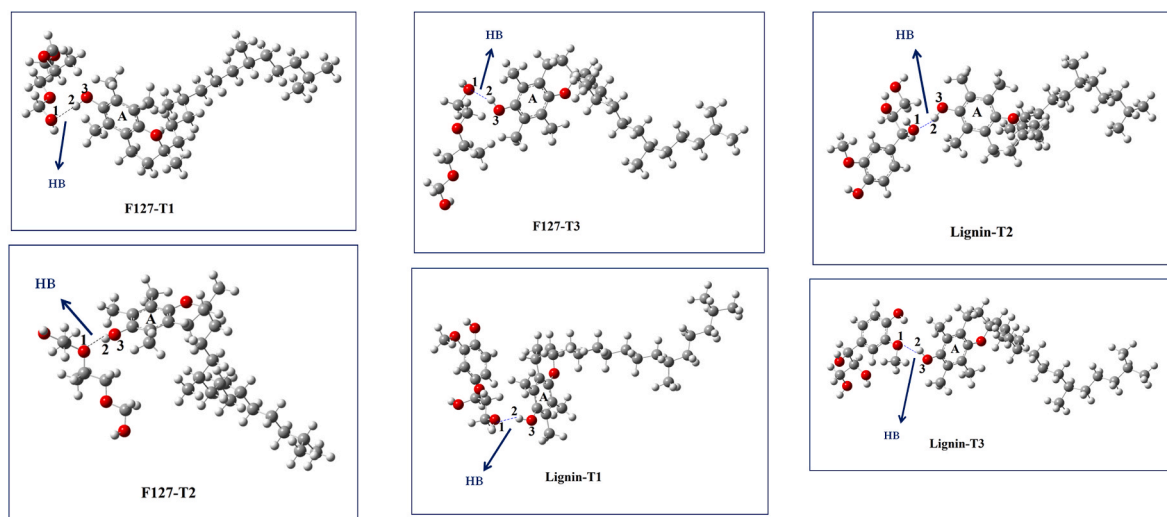

Fig. 1. The optimized structure of α-Tocopherol.

Fig. 2. Presentation of the hydrogen-bonded complexes that formed between surfactants and α-Tocopherol.

Table 1
Electronic data (in eV), binding energy values (in kcal mol^{-1}) and hydrogen bond lengths (in Å) of the complexes.

	[a]E_{HOMO}	[b]E_{LUMO}	[c]EG	[d]BE[a]	[e]d_{HB}
F127-T1	−4.818	0.410	5.228	11.93, *8.17*	1.965
F127-T2	−4.878	0.357	5.235	12.41, *10.06*	1.899
F127-T3	−4.795	0.387	5.182	12.40, *9.96*	1.885
Lignin-T1	−4.824	0.135	4.959	7.84, *5.83*	1.887
Lignin-T2	−4.770	0.075	4.846	11.65, *7.39*	1.840
Lignin-T3	−4.824	0.057	4.881	4.43, *4.22*	2.020

[a] The Italic values refer to BE values that obtained at the PBEKCIS/6–311++G (d,p) level of theory.

Interactions of valporic acid and F127 were formerly explored [20] that followed by formations of seven and six-member rings. The mentioned complexes have BE values comparable with the F127-T ones. Also, interactions of deferasirox (DFX) and F127 were previously studied [21] and results indicated that the hydrogen bonded F127-DFX complexes have smaller BE values than the F127-T ones. In another work, interplays between carfilzomib (CFZ) and F127 were examined [34]. The BE values of the F127-CFZ complexes are larger than F127-T ones. Thus, strengths of interactions in the hydrogen bonded F127-drug complexes are depending on the geometries and also affinities of the drugs to F127.

3.2. Atomic charges and aromaticity

Atomic charges of T and all complexes were calculated to find a relation between BE values of the complexes and the most important molecular descriptors in this view. Atomic charges of the atoms that take part in HB interactions, charge transfer (CT) and sum of atomic charges at six-member ring of T are listed in Table 2. The charge of atoms H_2 and O_3 in free T is 0.314 and −0.518 e, respectively. As shown in Table 2,

Table 2
Charge transfer (CT), charge of atoms that contribute in hydrogen bond interactions, and charge of six-member ring of α-Tocopherol.

	CT	q_{O1}	q_{H2}	q_{O3}	Q_A
F127-T1	−0.0439	−0.5314	0.3360	−0.6112	0.7104
F127-T2	−0.0348	−0.5313	0.3509	−0.6258	0.7012
F127-T3	−0.0469	−0.5477	0.3351	−0.6200	0.6967
Lignin-T1	−0.0650	−0.5628	0.3313	−0.6264	0.6885
Lignin-T2	−0.0434	−0.5535	0.3475	−0.6298	0.7072
Lignin-T3	−0.0364	−0.5876	0.3298	−0.6116	

positive charge of atom H_2 and negative charge of atom O_3 increase in the complexes in comparison to free T. Also, increase of atomic charges on atoms H_2 and O_1 in the complexes is followed by increase of BE values of the complexes. This result indicates that the strength of HB interactions can be influenced by alteration of charges of atoms that take part in such interplays.

Results indicate that the sum of atomic charges of T in all of the complexes is negative. Thus, there are charge transfers from F127 and lignin to T. Magnitude of charge transfers that occurred in the F127-T complexes is somewhat lesser than those in the Lignin-T ones. The sum of atomic charges at the ring A (Q_A) of free drug is 0.7188 e. Results show that Q_A values in the complexes decreased due to CT. Furthermore, increase of negative CT to ring A of T in the F127-T complexes is accompanied by increase of BE values. However, there is no such relationship in the case of Lignin-T complexes.

The NBO studies reveal that there are various electron charge transfers between molecular orbitals of the surfactants and T. These electron charge transfers can occur from molecular orbitals of surfactants (S) to T or vice versa. As reported in Table 3, the sum of stabilizing energies ($\sum E^{(2)}$) related to the electron charge transfers from molecular orbitals of F127 to T are larger than those for lignin to T. Moreover, the $\sum E^{(2)}$ values associated to the electron charge transfers from molecular orbitals of T to F127 are larger than those for T to lignin, too. Additionally, differences between donor-acceptor orbital energies (Ej-Ei) were surveyed. Results point out that behaviors of these values in the complexes are similar to $\sum E^{(2)}$ ones. Therefore, the $\sum E^{(2)}$ and (Ej-Ei) values have an effect on the different stability of the F127-T and Lignin-T complexes.

Aromaticity of the ring A in both free drug and all of the complexes was estimated using PDI benchmark [59]. The PDI value for the

Table 3
Sum of stabilizing energies and difference between donor-acceptor orbital energies related to the electron charge transfers between molecular orbitals of surfactants and α-Tocopherol.

	$\sum E^{(2)}$ S-T[a]	$\sum E^{(2)}$ T-S[b]	$\sum$(Ej-Ei) S-T	$\sum$(Ej-Ei) T-S
F127-T1	14.12	1.70	43.1	9.61
F127-T2	16.1	2.04	39.55	16.42
F127-T3	17.55	1.52	43.1	9.18
Lignin-T1	18.99	1.16	42.11	10.10
Lignin-T2	20.68	3.85	38.98	11.66
Lignin-T3	7.92	0.76	15.8	9.06

[a] Refers to surfactant to α-Tocopherol charge transfer.
[b] Refers to α-Tocopherol to surfactants charge transfer.

mentioned ring in the free drug is 0.08081 au. However, PDI value of this ring in the F127-T1, F127-T2, F127-T3, Lignin-T1, Lignin-T2, and Lignin-T3 complexes is 0.08096, 0.08107, 0.08067, 0.08113, 0.08094, and 0.08105 au, respectively. The change of aromaticity due to complex formation and the sum of PDI values for the F127-T complexes are lesser than those for the Lignin-T ones. As said, ring A plays a central role in the HB interaction and in each complex there is an overall CT from the surfactant to the drug. In fact, complex formation leads to alteration of properties of ring A. Results indicate that negative charges that are transferred to this ring in the F127-T complexes are smaller than those in the Lignin-T ones. This result implies that magnitudes of CT influence on the properties of the ring A, such as circulation of electrons and aromaticity. Consequently, formation of HB interactions in the F127-T complexes is accompanied by smaller negative CT to the ring A and lesser change of aromaticity in comparison to the Lignin-T ones. Thus, these effects provide good stability for the F127-T complexes.

3.3. AIM analyses

AIM studies were performed to discover relationship between properties of electron charge densities and BE values. Electron charge densities at each bond critical point (ρ_{BCP}) that formed between surfactants and T in the complexes are gathered in Table 4, showing that increase of the ρ_{BCP} values is followed by increase of BE values of the complexes. Kinetic electronic energy density (G(r)), potential electronic energy density (V(r)), total electronic energy density (H(r)) at bond critical points, Eigen values of Hessian matrix are also reported in Table 4. The intermolecular HB interactions in the current complexes are strong [60]. In addition, the product of electron charge densities and λ_2 at bond critical point for each complex is negative. Therefore, the HB interactions in these systems are attractive. It seems that directions of surfactants toward the drug may influence the strength of the mentioned interactions and affect the ρ_{BCP} values. Laplacian of electron charge density at each hydrogen bond critical point ($\nabla^2 \rho_{BCP}$) is also calculated. Sum of $\nabla^2 \rho_{BCP}$ values for the F127-T complexes is more negative than those for the Lignin-T ones. As said, HB interactions in the F127-T complexes are stronger in comparison to the Lignin-T counterparts.

3.4. LMO-EDA study

The localized molecular orbital energy decomposition analyses (LMO-EDA) [61] were executed to make a distinction between the contributions of the various components of interaction energy on the stability of the complexes. Interaction energy is comprised of electrostatic, exchange, repulsion, and polarization components that are symbolized as E_{elec}, E_{exch}, E_{rep}, and E_{pol}, respectively. These components are gathered in Table 5. As reported, E_{elec} is the most important component and has more contribution in the stability of the complexes than other components. Results also show that the sum of repulsion energies in the F127-T complexes is smaller in comparison to the Lignin-T ones. It seems that this effect plays an important role in improving stability of the mentioned complexes.

The relationship between the E_{elec} and ρ_{BCP} values was examined. The results suggest a linear correlation between the mentioned parameters with good linear correlation coefficient (R = 0.97) as follows:

Table 4
Properties of electron charge densities at hydrogen bond critical point of the complexes (au).

	ρ_{BCP}	$\nabla^2 \rho_{BCP}$	G(r)	V(r)	H(r)	λ_2
F127-T1	0.0284	−0.0242	0.0276	−0.0309	−0.0034	−0.0451
F127-T2	0.0327	−0.0260	0.0316	−0.0371	−0.0055	−0.0516
F127-T3	0.0352	−0.0269	0.0339	−0.0408	−0.0069	−0.0557
Lignin-T1	0.0348	−0.0255	0.0325	−0.0395	−0.0070	−0.0564
Lignin-T2	0.0386	−0.0263	0.0355	−0.0446	−0.0092	−0.0621
Lignin-T3	0.0208	−0.0231	0.0225	−0.0218	0.0006	−0.0299

Table 5
Components of interaction energies of the complexes in kcal mol^{-1}.

	E_{elec}	E_{exc}	E_{rep}	E_{pol}
F127-T1	−9.43	−8.56	16.04	−5.45
F127-T2	−12.29	−11.45	21.30	−5.75
F127-T3	−12.43	−11.14	20.67	−5.06
Lignin-T1	−12.22	−12.00	22.00	−5.40
Lignin-T2	−15.74	−13.69	25.35	−6.30
Lignin-T3	−6.65	−6.48	11.98	−3.32

$$E_{elec} = -476.33 \, \rho_{BCP} + 3.65 \qquad (4)$$

Therefore, electrostatic interactions play a fundamental role on the strengths of the intermolecular HB interactions in the F127-T and Lignin-T complexes.

3.5. DOS plots

Density of states (DOS) plots of the complexes is represented in Fig. 3. In these plots, frag 1 and frag 2 are related to the surfactants and drug, respectively. Results show that the contributions of drug in total density of states (TDOS) are higher than those of surfactants. The DOS plots are helpful to know the density of involvement of molecular orbitals in different energy levels.

As can be observed, the maximum in the mentioned plots are located in energy levels lower than HOMO level. In addition, energy levels related to the maximum TDOS for the F127-T complexes are lower than those for the Lignin-T ones. It seems that this difference in energy levels of the maximum TDOS has an effect on stability of these complexes.

3.6. Semi-empirical calculations

Semi-empirical methods utilize empirical corrections in order to improve performance of calculations. Semi-empirical calculations are parameterized to take in all thermochemical corrections. Moreover, semi-empirical methods recover some part of electron correlation effects due to parameterization with reference to experimental data. Heats of formation (ΔH_f values) of the complexes were calculated using AM1 method. The ΔH_f values for F127-T1, F127-T2, F127-T3, Lignin-T1, Lignin-T2, and Lignin-T3 are −392.806, −395.627, −391.182, −398.452, −399.015, and −400.809 kcal mol^{-1}, respectively. As can be seen, ΔH_f values of the F127-T complexes are less negative than those for the Lignin-T ones. Also, results indicate that the obtained hydrogen bond lengths using AM1 method are larger than those with DFT study. Indeed, d_{HB} values for the F127-T complexes are shorter than the Lignin-T structures. As said, BE values of the F127-T complexes are larger than those for the Lignin-T ones, which confirm the corresponding shorter d_{HB} values.

4. Conclusions

In this study, T-loaded microemulsions were designed using F127 and lignin surfactants by means of DFT computations. The O–H bond in the phenol ring of T is weaker than in most other phenols and acts as good hydrogen bond donor in the formation of HB interactions with surfactants. Binding energies of the F127-T complexes are larger than Lignin-T ones. The BE values of the F127-drug complexes are depending on the geometries and directions of drugs to surfactant. Also, hydrogen bond lengths in the F127-T complexes are shorter than those in the Lignin-T ones. There are negative charge transfers from surfactants to T. The sum of stabilizing energies related to CT from molecular orbitals of F127 to T is larger than that corresponding CT from lignin to T. Alteration of aromaticity owing to the formation of complexes and the sum of PDI values for the F127-T complexes are smaller than those for the Lignin-T ones. In fact, CT affects the circulation of electrons and
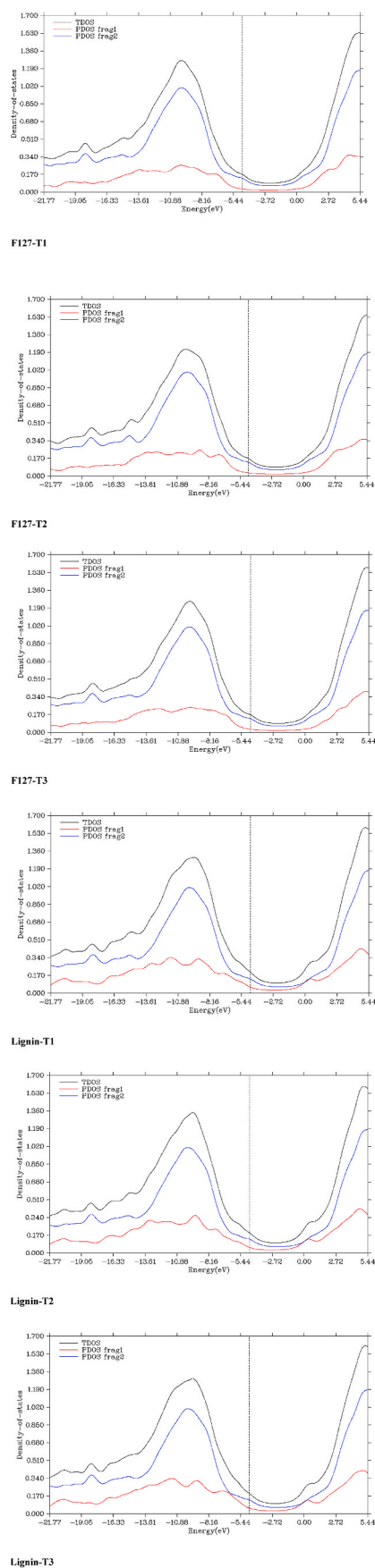
F127-T1

F127-T2

F127-T3

Lignin-T1

Lignin-T2

Lignin-T3

Fig. 3. Density of states (DOS) plots of the complexes.

aromaticity of phenol ring of T and influences the stability of the T-loaded microemulsions. The LMO-EDA studies show that the electrostatic interactions play a major role on stability of the complexes. Furthermore, the sum of repulsion energies in the F127-T complexes is smaller than those in the Lignin-T ones. The semi-empirical study points out that the ΔH_f values of the F127-T complexes are less negative than those for the Lignin-T ones.

CRediT authorship contribution statement

Pouya Karimi: Conceptualization, Investigation, Software, Visualization, Writing – original draft. **Abbas Rahdar:** Conceptualization, Methodology, Resources, Supervision, Writing – original draft. **Francesco Baino:** Validation, Writing – review & editing.

Declaration of competing interest

The authors declare that they have no known competing financial interests or personal relationships that could have appeared to influence the work reported in this paper.

Data availability

Data will be made available on request.

Acknowledgments

References

[1] J. Cieśla, M. Koczańska, J. Narkiewicz-Michałek, M. Szymula, A. Bieganowski, Alpha-tocopherol in CTAB/NaCl systems. The light scattering studies, J. Mol. Liq. 233 (2017) 15–22.

[2] J. Cieśla, M. Koczańska, J. Narkiewicz-Michałek, M. Szymula, A. Bieganowski, Effect of α-tocopherol on the properties of microemulsions stabilized by the ionic surfactants, J. Mol. Liq. 236 (2017) 117–123.

[3] Aditya Kumar, Ankush Prasad, Pavel Pospíšil, Formation of α-tocopherol hydroperoxide and α-tocopheroxyl radical: relevance for photooxidative stress in Arabidopsis, Sci. Rep. 10 (2020) 19646, https://doi.org/10.1038/s41598-020-75634-0.

[4] Q. Jiang, S. Christen, M.K. Shigenaga, B.N. Ames, gamma-tocopherol, the major form of vitamin E in the US diet, deserves more attention, Am. J. Clin. Nutr. 74 (2001) 714–722 [PubMed: 11722951].

[5] J. Ju, S.C. Picinich, Z. Yang, Y. Zhao, et al., Cancer-preventive activities of tocopherols and tocotrienols, Carcinogenesis 31 (2010) 533–542 [PubMed: 19748925].

[6] R. Brigelius-Flohe, F.J. Kelly, J.T. Salonen, J. Neuzil, et al., The European perspective on vitamin E: current knowledge and future research, Am. J. Clin. Nutr. 76 (2002) 703–716 [PubMed: 12324281].

[7] Aayushi Laliwala, Amita Daverey, Sandeep K. Agrawal, Alekha K. Dash, Alpha tocopherol loaded polymeric nanoparticles: preparation, characterizations, and in vitro assessments against oxidative stress in spinal cord injury treatment, AAPS PharmSciTech 23 (6) (2022) 195, https://doi.org/10.1208/s12249-022-02345-2.

[8] S. Srivastava, S. Gupta, S. Mohammad, I. Ahmad, Development of α-tocopherol surface-modified targeted delivery of 5-fluorouracil-loaded poly-D, L-lactic-co-glycolic acid nanoparticles against oral squamous cell carcinoma, J. Cancer Res. Therapeut. 15 (3) (2019) 480–490, https://doi.org/10.4103/jcrt.JCRT_263_18. PMID: 31169208.

[9] Carla Caddeo, Maria Letizia Manca, Josè Esteban Peris, Iris Usach, Octavio Diez-Sales, Maria Matos, Xavier Fernàndez-Busquets, Anna Maria Fadda, Maria Manconi, Tocopherol-loaded transfersomes: in vitro antioxidant activity and efficacy in skin regeneration, Int. J. Pharm. 551 (1–2) (2018) 34–41, https://doi.org/10.1016/j.ijpharm.2018.09.009.

[10] Youngjae Byun, Bong Hwang Jin, Hwan Bang Sung, Darby Duncan, Cooksey Kay, L. Paul, Dawson, Jin Park Hyun, Whiteside Scott, Formulation and characterization of α-tocopherol loaded poly ε-caprolactone (PCL) nanoparticles, LWT - Food Sci. Technol. (Lebensmittel-Wissenschaft -Technol.) 44 (2011) 24–28, https://doi.org/10.1016/j.lwt.2010.06.032.

[11] Melike Bayindir Bilgic, Nelisa Turkoglu Lacin, Hale Berber, Banu Mansuroglu, In vitro evaluation of alpha-tocopherol loaded carboxymethylcellulose chitosan copolymers as wound dressing materials, Materials Technology Advanced

Performance Materials 34 (2019) 386–393, https://doi.org/10.1080/10667857.2019.1573944.

[12] Lacey C. Simon, Rhett W. Stout, Cristina Sabliov, Bioavailability of orally delivered alpha-tocopherol by poly(lactic-Co-glycolic) acid (PLGA) nanoparticles and chitosan covered PLGA nanoparticles in F344 rats, Nanobiomedicine 3 (2016) 1–10, https://doi.org/10.5772/63305.

[13] Lamia Taouzinet, Sofiane Fatmi, Allaeddine Khellouf, Skiba Mohamed, Mokrane Iguer-ouada, Alpha tocopherol loaded in liposome: preparation, optimization, characterization and sperm motility protection, Drug Deliv. Lett. 10 (3) (2020) 228–236, https://doi.org/10.2174/2210303110666200302113209.

[14] Esra Metin, Pelin Mutlu, Ufuk Gündüz, Co-Delivery of doxorubicin and D-α-tocopherol polyethylene glycol 1000 succinate by magnetic nanoparticles, Anti Cancer Agents Med. Chem. 18 (8) (2018) 1138–1147, https://doi.org/10.2174/1871520618666180313154724.

[15] Fabíola Garcia Praça, Juliana Santos Rosa Viegas, Hong Yong Peh, Tuane Nardacchione Garbin, Wanessa Silva Garcia Medina, Maria Vitoria Lopes Badra Bentley, Mater. Sci. Eng. C 110 (2020) 110639, https://doi.org/10.1016/j.msec.2020.110639.

[16] A. Rey-Rico, J. Frisch, J.K. Venkatesan, G. Schmitt, I. Rial-Hermida, P. Taboada, et al., PEO-PPO-PEO carriers for rAAV-mediated transduction of human articular chondrocytes in vitro and in a human osteochondral defect model, ACS Appl. Mater. Interfaces 8 (32) (2016) 20600–20613.

[17] J. Tao, Q. Zhu, F. Qin, M. Wang, J. Chen, Z.-P. Zheng, Preparation of steppogenin and ascorbic acid, vitamin E, butylated hydroxytoluene oil-in-water microemulsions: characterization, stability, and antibrowning effects for fresh apple uice, Food Chem. 224 (2017) 11–18.

[18] D.S. Sisson, J.A.V. Morais, Í.A. Vanderlei, A.S. Santos, R.B. Azevedo, L.A. Muehlmann, J.P. Longo, Oral delivery of fish oil in oil-in-water nanoemulsion: development, colloidal stability and modulatory effect on in vivo inflammatory induction in mice, Biomed. Pharmacother. 133 (2021) 110980.

[19] M. Ali Aboudzadeh, Ehsan Mehravar, Mercedes Fernandez, Luis lezama, and radmila tomovska, low-energy encapsulation of α-tocopherol using fully food grade oil-in-water microemulsions, ACS Omega 3 (2018) 10999–11008, https://doi.org/10.1021/acsomega.8b01272.

[20] Anayatollah Salimi, et al., Development and evaluation of azelaic acid-loaded microemulsion for transfollicular drug delivery through guinea pig skin: A mechanistic study, Adv. Pharm. Bull. (2020) 239, https://doi.org/10.34172/apb.2020.028.

[21] Nafiseh Jirofti, et al., Polymer stabilized, phenytoin-loaded nanomicelles as promising nanocarriers: In silico and in vitro evaluations, Eur. Polym. J. 196 (2023) 112228.

[22] R. Basak, R. Bandyopadhyay, Encapsulation of hydrophobic drugs in pluronic F127 micelles: effects of drug hydrophobicity, solution temperature, and pH, Langmuir 29 (13) (2013) 4350–4356.

[23] F.A. Maulvi, A.R. Desai, H.H. Choksi, R.J. Patil, K.M. Ranch, B.A. Vyas, et al., Effect of surfactant chain length on drug release kinetics from microemulsion-laden contact lenses, Int. J. Pharm. 524 (1–2) (2017) 193–204.

[24] M. Gallarate, M.E. Carlotti, M. Trotta, E. Ugazio, Disperse systems as topical formulations containing α-tocopherol, J. Drug Deliv. Sci. Technol. 14 (6) (2004) 471–477.

[25] B. Rozman, M. Gasperlin, E. Tinois-Tessoneaud, F. Pirot, F. Falson, Simultaneous absorption of vitamins C and E from topical microemulsions using reconstructed human epidermis as a skin model, Eur. J. Pharm. Biopharm. 72 (1) (2009) 69–75.

[26] M.A. James-Smith, D. Shekhawat, S. Cheung, B.M. Moudgil, D.O. Shah, Role of ethylene oxide and propylene oxide groups of Pluronics in binding of fatty acid to Pluronics in microemulsions, J. Surfactants Deterg. 11 (3) (2008) 237–242.

[27] S.F. Khattak, S.R. Bhatia, S.C. Roberts, Tissue Eng. 11 (2005) 974.

[28] P. Dehghan Kelishady, E. Saadat, F. Ravar, H. Akbari, F. Dorkoosh, Pluronic F127 polymeric micelles for co-delivery of paclitaxel and lapatinib against metastatic breast cancer: preparation, optimization and in vitro evaluation, Pharmaceut. Dev. Technol. 20 (8) (2015) 1009–1017.

[29] M. Ramakanta, G. Narayani, M. Saptarshi, Enhanced Binding of Phenosafranin to Triblock Copolymer F127 Induced by Sodium Dodecyl Sulfate: A Mixed Micellar System as an Efficient Drug Delivery Vehicle, 2016.

[30] X. Meng, J. Liu, X. Yu, J. Li, X. Lu, T. Shen, Pluronic F127 and D-α-tocopheryl polyethylene glycol succinate (TPGS) mixed micelles for targeting drug delivery across the blood brain barrier, Sci. Rep. 7 (1) (2017) 2964.

[31] H. Wang, G.R. Williams, J. Wu, J. Wu, S. Niu, X. Xie, S. Li, L.-M. Zhu, Pluronic F127-based micelles for tumor-targeted bufalin delivery, Int. J. Pharm. 559 (2019) 289–298.

[32] Abbas Rahdar, et al., The synthesis of methotrexate-loaded F127 microemulsions and their in vivo toxicity in a rat model, J. Mol. Liq. 313 (2020) 113449.

[33] A. Rahdar, P. Hasanein, M. Bilal, H. Beyzaei, G.Z. Kyzas, Quercetin-loaded F127 nanomicelles: antioxidant activity and protection against renal injury induced by gentamicin in rats, Life Sci. 276 (2021) 119420.

[34] Salwa Shaarani, Shahrul Sahul Hamid, Kaus Noor Haida Mohd, The Influence of pluronic F68 and F127 nanocarrier on physicochemical properties, in vitro release, and antiproliferative activity of thymoquinone drug, Pharmacognosy Res. 9 (1) (2017) 12.

[35] R.G. Saratale, A comprehensive overview and recent advances on polyhydroxyalkanoates (PHA) production using various organic waste streams, Bioresour. Technol. 325 (2021) 124685.

[36] P. Figueiredo, In vitro evaluation of biodegradable lignin-based nanoparticles for drug delivery and enhanced antiproliferation effect in cancer cells, Biomaterials 121 (2017) 97.

[37] H. Li, Preparation of nanocapsules via the self-assembly of kraft lignin: a totally green process with renewable resources, ACS Sustain. Chem. Eng. 4 (2016) 1946.

[38] E. Chiani, A. Beaucamp, Y. Hamzeh, M. Azadfallah, A. Thanusha, M.N. Collins, Synthesis and characterization of gelatin/lignin hydrogels as quick release drug carriers for Ribavirin, Int. J. Biol. Macromol. 224 (2023) 1196–1205.

[39] K. Pathania, S.P. Sah, D.B. Salunke, M. Jain, A.K. Yadav, V.G. Yadav, S.V. Pawar, Green synthesis of lignin-based nanoparticles as a bio-carrier for targeted delivery in cancer therapy, Int. J. Biol. Macromol. 229 (2023) 684–695.

[40] Y. Zhou, Effects of lignin-based hollow nanoparticle structure on the loading and release behavior of doxorubicin, Materials 12 (2019) 1694.

[41] Y. Zhou, Preparation of targeted lignin–based hollow nanoparticles for the delivery of doxorubicin, Nanomaterials 9 (2019) 188.

[42] Y.H. Deng, Hollow lignin azo colloids encapsulated avermectin with high anti-photolysis and controlled release performance, Ind. Crop. Prod. 87 (2016) 191.

[43] Y. Li, pH-responsive lignin-based complex micelles: preparation, characterization and application in oral drug delivery, Chem. Eng. J. 327 (2017) 1176.

[44] Abbas Rahdar, Saman Sargazi, Barani Mahmood, Sheida Shahraki, Fakhara Sabir, M. Ali Aboudzadeh, Lignin-stabilized doxorubicin microemulsions: synthesis, physical characterization, and in vitro assessments, Polymers 13 (2021) 641, https://doi.org/10.3390/polym13040641.

[45] P. Karimi, A. Ebrahimi, Investigation of interactions of benzene molecule and sodium ions with modeled carbon nanotubes as drug delivers, J. Appl. Res. Chem. 10 (2016) 73–83.

[46] M.J. Frisch, G.W. Trucks, H.B. Schlegel, G.E. Scuseria, M.A. Robb, J.R. Cheeseman, G. Scalmani, V. Barone, B. Mennucci, G.A. Petersson, H. Nakatsuji, M. Caricato, X. Li, H.P. Hratchian, A.F. Izmaylov, J. Bloino, G. Zheng, J.L. Sonnenberg, M. Hada, M. Ehara, K. Toyota, R. Fukuda, J. Hasegawa, M. Ishida, T. Nakajima, Y. Honda, O. Kitao, H. Nakai, T. Vreven, J.A. Montgomery, J.E. Peralta Jr., F. Ogliaro, M. Bearpark, J.J. Heyd, E. Brothers, K.N. Kudin, V.N. Staroverov, R. Kobayashi, J. Normand, K. Raghavachari, A. Rendell, J.C. Burant, S.S. Iyengar, J. Tomasi, M. Cossi, N. Rega, J.M. Millam, M. Klene, J.E. Knox, J.B. Cross, V. Bakken, C. Adamo, J. Jaramillo, R. Gomperts, R.E. Stratmann, O. Yazyev, A.J. Austin, R. Cammi, C. Pomelli, J.W. Ochterski, R.L. Martin, K. Morokuma, V.G. Zakrzewski, G.A. Voth, P. Salvador, J.J. Dannenberg, S. Dapprich, A.D. Daniels, O. Farkas, J.B. Foresman, J.V. Ortiz, J. Cioslowski, D.J. Fox, Gaussian 09, Revision A.02, Gaussian, Inc., Wallingford CT, 2009.

[47] Li Rao, Hongwei Ke, Gang Fu, Xin Xu, Yijing Yan, Performance of several density functional theory methods on describing hydrogen-bond interactions, J. Chem. Theor. Comput. 5 (1) (2009) 86–96, https://doi.org/10.1021/ct800237n.

[48] Marek Lozynski, Danuta Rusinska-Roszak, Hans-Georg Mack, Hydrogen bonding and density functional calculations: the B3LYP approach as the shortest way to MP2 results, J. Phys. Chem. A 102 (17) (1998) 2899–2903, https://doi.org/10.1021/jp973142x.

[49] R.F.W. Bader, in: Atoms in Molecules: A Quantum Theory, Oxford University Press, Oxford, 1990.

[50] A.E. Reed, L.A. Curtiss, F.J. Weinhold, Intermolecular interactions from a natural bond orbital, donor-acceptor viewpoint, Chem. Rev. 88 (1998) 899–926, https://doi.org/10.1021/cr00088a005.

[51] E.D. Glendening, A.E. Reed, J.E. Carpenter, F. Weinhold, NBO Version 3.1, Gaussian Inc., Pittsburgh, 2003.

[52] J. Poater, X. Fradera, M. Duran, M. Solà, The delocalization index as an electronic aromaticity criterion: application to a series of planar polycyclic aromatic hydrocarbons, Chem. Eur J. 9 (2003) 400–406.

[53] M.J.S. Dewar, E.G. Zoebisch, E.F. Healy, AM1: a new general purpose quantum mechanical molecular model, J. Am. Chem. Soc. 107 (1985) 3902–3909.

[54] G.W. Burton, K.U. Ingold, Autoxidation of biological molecules. 1. Antioxidant activity of vitamin E and related chain-breaking phenolic antioxidants in vitro, J. Am. Chem. Soc. 103 (21) (1981) 6472–6477, https://doi.org/10.1021/ja00411a035.

[55] Pouya Karimi, Effects of structure and partially localization of the π electron clouds of single-walled carbon nanotubes on the cation-π interactions, Iran, J. Chem. Chem. Eng. 35 (2016) 35–43.

[56] K.A. Wilson, D. Holland, S.D. Wetmore, Topology of RNA-Protein Nucleobase-Amino Acid p–p Interactions and Comparison to Analogous DNA–protein p–p contacts, RNA 22 (5) (2016) 696–708.

[57] P. Karimi, Investigation of simultaneous cation-π and π-π stacking interactions on graphene and some bend graphenes as curved surfaces of carbon nanohorns, J. Struct. Chem. 59 (2018) 1137–1143.

[58] Pouya Karimi, Mahmood Sanchooli, Fatemeh Shojaa-Hormozzahi, Estimation of resonance assisted hydrogen bond (RAHB) energies using properties of ring critical points in some dihydrogen-bonded complexes, J. Mol. Struct. 1242 (2021) 130710.

[59] Pouya Karimi, Mahmoud Sanchooli, Tuning the resonance-assisted hydrogen bond (RAHB) of malonaldehyde using π-conjugated substituents and presentation of its energy decomposition, J. Mol. Graph. Model. 112 (2022) 108142.

[60] Isabel Rozas, Ibon Alkorta, José Elguero, JACS 122 (2000) 11154–11161.

[61] Maximillian J.S. Phipps, Thomas Fox, Christofer S. Tautermann, Chris-Kriton Skylaris, Energy decomposition analysis approaches and their evaluation on prototypical protein–drug interaction patterns, Chem. Soc. Rev. 44 (2015) 3177–3211.